# A Method Combining Mobile Transmissometer and Lidar for High Precision Measurement of Visibility

Meng Li and Guojin Wang

***Abstract*—High precision measurement of visibility has wide applications in the fields of civil aviation and maritime transportation. However, for a long time, the non-uniform of the atmosphere and optical contamination under low visibility have always been important issues affecting the measurement accuracy of visibility. This paper proposes a novel method that combines a mobile transmissometer with Lidar, which can not only accurately measure visibility in non-uniform atmospheric environments, but also effectively suppress environmental contamination by using the method of single end sampling. In this method, the mobile transmissometer is coupled with the Lidar at its baseline end, thereby effectively improving the Lidar measurement accuracy with the high-precision measurement results of the mobile transmissometer. The experimental and simulation results demonstrate that this method has better performances of anti noise and optical contamination suppression, compared to traditional Lidar and atmospheric transmissometer. It can achieve high-precision visibility measurement in a large range of non-uniform atmospheric environments, and also exhibits good robustness in low visibility environments.**

***Index Terms*—Visibility, mobile transmissometer, Lidar.**

## I. Introduction

ATMOSPHERIC visibility, as an important meteorological parameter, is widely employed in fields of road transportation, navigation and civil aviation [1], [2]. At present, visibility measurement methods mainly involve transmission, forward scattering, as well as backward scattering [3], [4], [5]. However, for high-precision visibility measurements, only the transmission method is extensively applied, due to its perfect compliance with human visual principles and excellent suppression of optical noise [6], [7], [8]. But in practical applications, there are always two important issues in high-precision measurement of visibility with the transmission method.

Firstly, it is difficult to accurately measure non-uniform atmospheric environments. The transmissometer can only provide average visibility in a certain space, due to its sampling type of fixed baseline. In addition, because of its limited sampling space, it is difficult to cover a larger spatial range. The existing methods mainly combine transmission visibility meters at multiple different locations for measurement [9], [10], [11]. For example, the World Meteorological Organization (WMO) conducted a combined measurement experiment using 14 transmissometers [7]; The Royal Dutch Meteorological Agency calibrated atmospheric visibility transmissometer of different baseline lengths; Hong Kong Observatory applied three atmospheric transmissometers to jointly measure regional visibility. Although this method can to some extent solve the measurement problem of non-uniform atmosphere, the number of visibility meters that can be installed is limited and cannot cover all demand areas well. Additionally, for areas where visibility meters cannot be installed, such as airport runways or specific high altitudes, this method is still ineffective.

Secondly, the optical lens contamination caused by aerosol environment can also affect the accuracy of visibility measurement, due to the inconsistency of light intensity errors between the transmitting and receiving ends, which is difficult to avoid through optical design. Therefore, in practical applications, the transmission method often establishes a contamination error correction model that evolves over time for visibility calculation [12], [13], and is fully obtained through practical experience. Although this method can to some extent suppress the accumulation effect of contamination errors, due to the strong regional differences in aerosol environments, the effectiveness of this model varies in different environments. In addition, calibration of multiple visibility meters is also a means of correcting optical contamination errors. For example, Vaisal's transmissive visibility meter applies forward scattering meters to correct the optical contamination errors. This approach mainly focuses on error correction for high visibility, but still does not perform well in low visibility ranges.

In theory, among all visibility measurement methods, Lidar is the best method to address the above two issues [14], [15]. Due to its infinitely long measurement baseline, the extinction coefficient of the entire optical path can be obtained through inversion calculation, thus visibility in non-uniform atmospheric environments can be measured effectively. Due to the design of receiving and transmitting at the same end, mirror contamination errors can be offset. Although Lidar has the above advantages, in practical applications, it has always been difficult to achieve a measurement accuracy of less than 10% for atmospheric

Manuscript received 11 April 2024; revised 29 May 2024; accepted 3 June 2024. Date of current version 13 June 2024. This work was supported in part by the Scientific Research Program of Tianjin Municipal Education Commission under Grant 2021KJ033, in part by the National Key R&D Program of China under Grant 2020YFB1600101 and Grant 2020YFB1600103, and in part by the Fundamental Research Funds for the Central Universities, China, under Grant 3122022QD11. *(Corresponding author: Meng Li.)*

Meng Li is with the Key Laboratory of Operation Programming & Safety Technology of Air Traffic Management, Civil Aviation University of China, Tianjin 300300, China (e-mail: m-li@cauc.edu.cn).

Guojin Wang is with the Key Laboratory of Operation Programming & Safety Technology of Air Traffic Management, Civil Aviation University of China, Tianjin 300300, China.

Digital Object Identifier 10.1109/JPHOT.2024.3410293

transmissometer, due to strong background noise of Lidar and difficulty in accurately estimating boundary values.

For denoising Lidar signal, many types of methods have been proposed, such as sliding average method, frequency decomposition method, assimilation filtering method, and joint filtering denoising method [16], [17], [18], [19], [20]. Among them, the frequency decomposition method decomposes and denoises the Lidar signal in terms of frequency characteristics, such as wavelet analysis [21], Fourier decomposition [22], and empirical mode decomposition [23]. This type of related researches is the most extensive, and its core purpose is to adapt to the nonlinear and non-stationary characteristics of Lidar signals. The assimilation filtering method uses approaches such as ensemble Kalman filtering and particle filtering for signal denoising, taking into account the constraints of Lidar physical equations. In addition, researchers have proposed many combined algorithms of multiple methods for denoising Lidar signal, including morphological filtering and empirical mode decomposition [24], soft thresholding and ensemble empirical mode decomposition [25], complementary ensemble empirical mode decomposition and wavelet thresholding [26], and so on. However, because these methods are still based on a general noise model and lack prior analysis of signal features, their denoising effect is not ideal.

For boundary value calculation, the Kell method is currently the most classic method in the field of visibility measurement. In order to improve noise resistance and computational efficiency, researchers have proposed various methods based upon Kell method [27], such as using fixed point method [28], improved Newton method [29], joint Broyden algorithm and least squares method [30]; Two way transmittance method [31]. In recent years, with the development of hardware technology, the joint observation methods have gradually become an important method for inverting visibility extinction coefficients, for reason that they can calculate boundary values more accurately through joint measurements. For example, In multi-channel Mi-Raman scattering Lidar, the boundary values are directly inverted using Raman radar channels [32]; Using millimeter wave radar and dual wavelength Lidar, boundary values were calculated through joint algorithm inversion [33]; The atmospheric transmissometer and Lidar are used to measure visibility, and the measurement results of the atmospheric transmittance meter are directly used as boundary values [34]. However, existing research still lacks accuracy in measuring and calculating boundary values. Even if combined observation methods are used to calculate boundary values, new measurement errors may still be introduced. For example, when applying Raman scattering Lidar, the noise resistance of Raman Lidar should also be considered; The combination of Lidar and traditional atmospheric transmission instruments can only determine the boundary value based on the average extinction coefficient, and cannot apply the accurate distribution of extinction coefficients. At the same time, the optical pollution problem of traditional transmission instruments also needs to be considered.

This article proposes a visibility measurement method using a combination of Lidar and a mobile transmissometer to address the aforementioned issues. This method uses Lidar as the main body for visibility measurement, and uses high-precision measurement of a mobile transmissometer to couple and correct it. For the denoising of Lidar, the high-precision measurement results of a transmissometer is applied as a clean sample to denoise the Lidar, which can effectively solve the problem of lacking prior information. For the calculation of Lidar boundary values, the mobile transmissiometer can obtain an accurate distribution of extinction coefficients, which are used to calculate the boundary values for improving calculation accuracy of visibility. Additionally, due to the single end moving measurement method adopted by the mobile transmissiometer, only the light intensity at the receiving end is considered in the calculation, which can effectively avoid measurement errors caused by inconsistent optical pollution between the transmitting end and the receiving end.

## II. System and Method

The entire system consists of a mobile transmissometer and a Lidar, as shown in Fig. 1 . The mobile transmissometer is a high-precision measurement unit, and its obtained visibility values can be used for background noise removal and boundary value inversion calculation in Lidar measurement systems. The entire method is as follows.

### A. Mobile Atmospheric Transmissometer Measurement

As shown in Figs. 1 and 2. Mobile atmospheric transmissometer consists of a laser emission unit, an optical receiving unit, a sliding track unit, an trolley unit, and a control and data processing unit.The laser emission unit includes a laser, an emission optical path system, and an adjustment bracket. The laser is expanded through the emission optical path system and emitted along the orbital direction with 532 nm green light, a divergence angle of$<$1.5 mrad and a spot diameter of 2mm. The position and direction of the laser beam can be changed by manually adjusting the emission unit adjustment bracket. The optical receiving unit consists of an optical chopper, a photodetector, a lock-in amplifier, and a receiving optical system. The aperture size of the chopper determines the size of the collimated light received. Continuous laser passes through a chopper, enters a lock-in amplifier, and is finally received by a photodetector, which can effectively suppress optical noise.The high-precision sliding track unit is composed of two 55 m long steel guide rails with a spacing of 0.35 m between the guide rails and a height of 0.2 m. An electromagnetic induction plate is installed every 5 m beside the guide rail to calibrate the detection distance. The trolley can move smoothly on the guide rail with a distance error of less than 0.005 m. The trolley unit consists of a bottom plate, a car cover, rollers, gears, servo motors, reducers, programmable logic controllers, proximity sensors, and inverters.A photoelectric receiving unit and a signal acquisition unit are placed on the bottom plate. The trolley is placed on a guide rail, and the PLC controls the trolley's motion speed, round trip frequency, and dwell time through the operation of the servo motor.Based on the signal from the proximity sensor, the position of the car can be detected. During the movement of the trolley, the deviation in the X/Y direction is extremely low, ensuring that the receiving probe

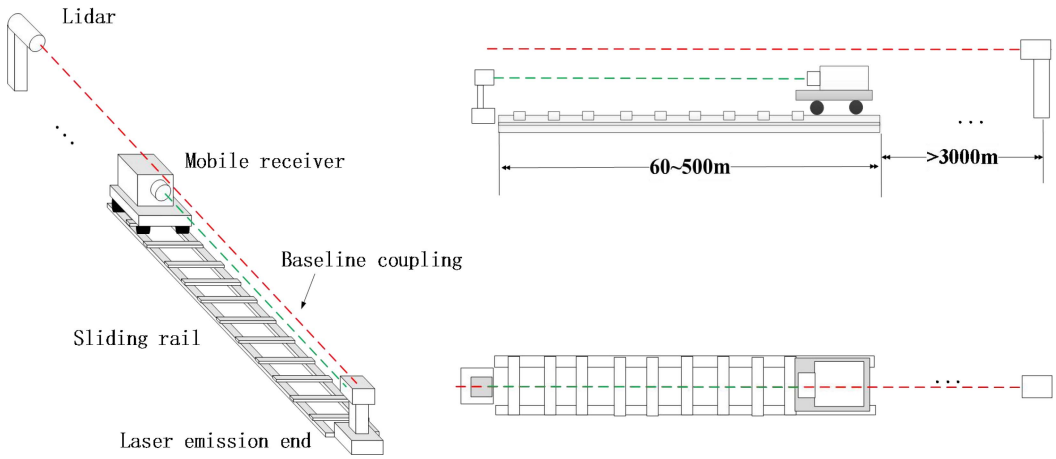


Fig. 1. Oblique view (left), side view (top right), and top view (bottom right) of the combination of Lidar and mobile transmissometer.

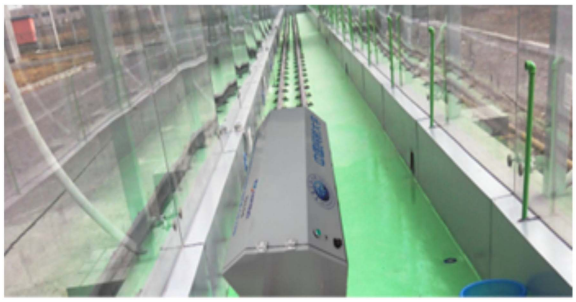

Fig. 2. Mobile transmissometer for visibility measurement.

is always in the effective receiving optical path. The control and data processing unit includes an embedded industrial computer, which analyzes and processes the received signals through software, and controls the photoelectric receiving components and PLC working status. To ensure signal stability, the entire system adopts wired transmission.

### *B. Lidar System*

The Lidar visibility meter adopts a Y-shaped fiber bundle that integrates transmission and reception to achieve coaxial design, with a Cassegrain telescope serving as both an optical signal transmitter and receiver. As shown in Fig. 3, the system consists of three parts: a laser emitting unit, an optical receiving unit, and a signal detection and data acquisition unit. The laser emission unit uses a diode pumped Nd… YAG532nm laser as the light source, which is close to the most sensitive 550 nm of the human eye, so its measured atmospheric level visibility can be well combined with human vision. The laser beam emitted by the laser is coupled into the emitting fiber through a fiber coupler, collimated and expanded, and then horizontally projected into the atmosphere through a telescope. Backscattered light is received by the same telescope, and the obtained optical signal is focused and coupled into the 8 outer receiving fibers of the fiber bundle. The received signal is transmitted through the receiving fibers and the background light is removed through a narrowband

Fig. 3. Lidar for visibility measurement.

TABLE I
THE MAIN TECHNICAL PARAMETERS OF THE LIDAR

| Item | Parameter |
|---|---|
| Transmitter | Nd YAG 532nm |
| Pulse energy | 30μJ |
| Repetition frequency | 2000Hz |
| Pulse duration | 9ns |
| Divergence | 0.5mrad |
| Receiver telescope | Cassegrain |
| Diameter | 203mm |
| NA of fiber | 0.22 |
| Detector | PMT |
| Data acquisition | Photo counter |
| Range resolution | 7.5m |

interference filter. The signal is detected by a photomultiplier tube (PMT) and collected by a photon counter. Finally, it is sent to a computer for signal storage and subsequent analysis. The effective horizontal detection range of the micro pulse Lidar system is 4 km during the day and 14 km at night.

Table I presents the main technical parameters of the Lidar. The emission wavelength, repetition frequency, and pulse energy of the laser are 532 nm, 2000 Hz, and 30 $\mu$J, respectively, which

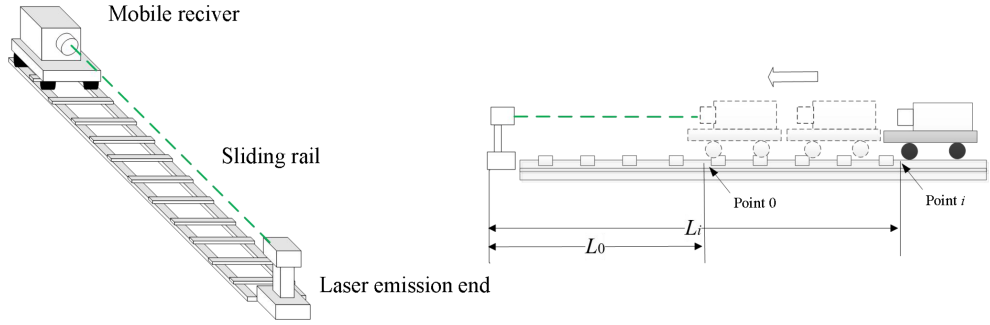


Fig. 4. Oblique view (left) and side view (right) of the mobile transmissometer.

meet the safety requirements of the human eye. Due to the weak echo signal and low output current of PMT, the analog acquisition mode can no longer function properly. Therefore, single photon counting mode is adopted here.

### C. Measurement Method of Mobile Transmissometer

The system can measure the laser signal at point *i* by moving the receiving end, and according to the Beer Lambert law, a laser atmospheric attenuation model can be expressed as:

$$\eta_i I_i = \eta_0 I_0 \exp\left(-\int_{L_0}^{L_i} \sigma\left(L\right) dL\right) \tag{1}$$

where, $\eta_i$and $\eta_0$ represent the lens contamination errors of the mobile receiver at the final point *i* and initial point 0 (in Fig. 4), respectively. $L_i$ and $L_0$ indicate the movement distance of the mobile receiver at the final point *i* and initial point 0, respectively. $\sigma$ is the extinction coefficient.

For the traditional transmissometer, due to the different lens contamination errors at the transmitting and receiving ends, namely $\eta_i \neq \eta_0$, a proportional error $\eta_i/\eta_0$ in the calculated extinction coefficient will be introduced. However, for our proposed system, because only a single mobile receiver is used, the lens contamination error at the receiving end can be considered constant, namely $\eta_i = \eta_0$. Therefore, the pollution error can be offset, which is the biggest advantage of mobile measurement methods, compared to the traditional transmissometer with fixed receiving end. In this case, it can be obtained that:

$$I_i = I_0 \exp\left(-\int_{L_0}^{L_i} \sigma\left(L\right) dL\right). \tag{2}$$

Thus, the relationship model between the extinction coefficient $\sigma$ and final movement distance $L_i$can be expressed as:

$$\sigma\left(L_i\right) = -\frac{d\left(\ln\left(I_i\left(L_i\right)/I_0\right)\right)}{dL_i}. \tag{3}$$

Then, according to the reference [35], visibility can be calculated as:

$$V\left(L_i\right) = \frac{Cg\left(\lambda\right)}{\sigma\left(L_i\right)} \tag{4}$$

where $q$ is the correction factor, usually taken as 3, and $\lambda$ is the emission spectrum. Based on experience, $g(\lambda)$can be expressed as:

$$g\left(\lambda\right) = \left(\frac{0.55}{\lambda}\right)^q;\ q = \begin{cases} 0.585V^{\frac{1}{3}} & V < 6\text{km} \\ 1.3 & 6\text{km} \leq V < 50\text{km} \\ 1.6 & V \geq 50\text{km} \end{cases}. \tag{5}$$

### D. Inversion Calculation of Lidar Under Coupled Mobile Transmissometer

Two primary challenges hinder the use of Lidar in high-precision visibility measurement. Firstly, the influence of background noise arises from a long baseline and a large sampling volume. Secondly, accurately calculating the boundary value of the extinction coefficient poses a difficulty. In the system proposed in this project, a period of high-precision extinction coefficient measurement over 50 m is attainable through mobile high-precision measurement. This measurement can be coupled with the Lidar signal, enhancing the accuracy of the inversion measurement result. The empirical mode decomposition, known for its adaptability and ability to handle nonlinear and non-stationary signals such as Lidar signals without requiring predefined basis functions, is employed. Consequently, an inversion calculation method based upon empirical mode decomposition is proposed for calculating atmospheric visibility, and demonstrated in Fig. 5.

1) The signals acquired by the Lidar are decomposed into multiple intrinsic mode functions using the empirical mode decomposition. The upper and lower envelopes are employed to fit the Lidar distance-corrected signal $s_0$, and the mean of upper and lower envelopes is calculated, termed as $m_1$. Subsequently, we subtract $m_1$ from the signal $s_0$ to obtain a new signal $s_1$. if $s_1$satisfies the condition:

$$\frac{\left(s_0 - s_1\right)^2}{{s_0}^2} < \Delta. \tag{6}$$

it is defined as the intrinsic mode function (IMF) $c_1$; otherwise, it is set as an original signal, and enters the initial step again. ($\Delta$ is the value of standard deviation coefficient.) The iterative process $s_i - m_{i+1} = s_{i+1}$ is repeated *K* times until $s_i$ satisfies the condition described by (6), termed as IMF $c_1$. We subtract $c_1$ from the signal $s_0$ to generate a new signal, which is reset as $s_0^1$ for a new iteration of the initial step. Then, $c_2$can be obtained. This iterative process continues until the signal $s_0$satisfies

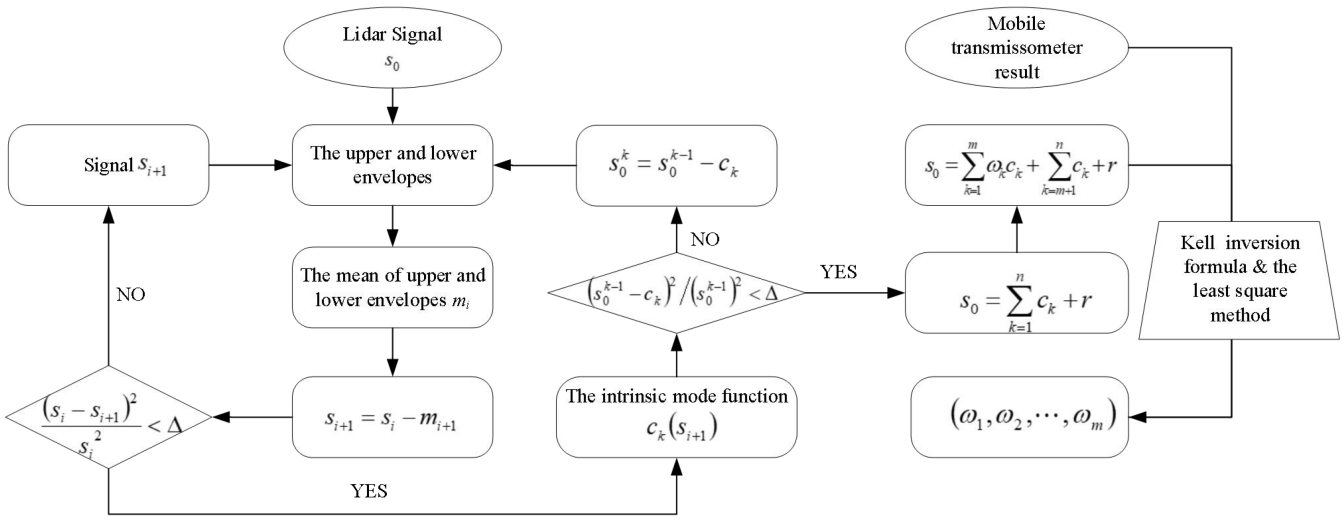


Fig. 5. The flowchart of Lidar signal decomposition and reconstruction.

$(s_0^{k-1} - c_k)^2 / (s_0^{k-1})^2 < \Delta$ or becomes a monotonic function, termed as $r$. Finally, The result of empirical mode decomposition can be expressed as:

$$s_0 = \sum_{k=1}^{n} c_k + r. \tag{7}$$

2) By setting a weight coefficient $\omega_k$ for each IMF, the reconstruction equation of the original signal can be obtained:

$$s_0 = \sum_{k=1}^{n} \omega_k c_k + r. \tag{8}$$

The denoising of Lidar signal can be realized by changing the weight coefficient $\omega_k$. It is assumed that the first $m$ weight coefficients are variable weight coefficients, and the reconstruction equation can be expressed as follows:

$$s_0 = \sum_{k=1}^{m} \omega_k c_k + \sum_{k=m+1}^{n} c_k + r. \tag{9}$$

3) High-precision visibility measurement results can be represented in discrete form as $\sigma_{l_i}$ $(i = 1, 2, \cdots, k)$, where the measurement points correspond to those of the Lidar, with a discrete interval equal to the Lidar's distance resolution. Because the Lidar's boundary values correspond to high-precision measurement results $\sigma_k$, based upon the Kell inversion formula, the inverted signal for the Lidar extinction coefficient can be expressed as:

$$\sigma' = \frac{\exp\left\{\left[s_0(l) - s_0(l_k)\right]/q\right\}}{\frac{1}{\sigma_{l_k}} + \frac{2}{q}\int_l^{l_c} \exp\left\{\left[s_0(l') - s_0(l_k)\right]/q\right\} dl'}. \tag{10}$$

$q$ is a coefficient related to the Lidar wavelength, aerosol refractive index, and particle size distribution, with a range of $0.67 \le q \le 1$. $l$ is the detection distance of the Lidar, $l_k$is the boundary distance corresponding to the measurement points of $\sigma_{l_k}$.Bringing (9) into (10), we can obtain the Lidar extinction coefficient inversion model $\sigma'(\omega_1, \omega_2, \cdots, \omega_m, l)$ based on weighting coefficients. Finally, the least square model is established based upon the discrete values of high-precision measurement results $\sigma_{l_i}$ $(i = 1, 2, \cdots, k)$ and the Lidar inversion model $\sigma'(\omega_1, \omega_2, \cdots, \omega_m, l)$:

$$f(\omega_1, \omega_2, \cdots, \omega_m) = \sum_{j=1}^{k} \left(\sigma'(\omega_1, \omega_2, \cdots, \omega_m, l_j) - \sigma_{l_j}\right)^2 \tag{11}$$

when $f(\omega_1, \omega_2, \cdots, \omega_m)$ takes the minimum value, the corresponding weight coefficient $(\omega_1, \omega_2, \cdots, \omega_m)$ is the reconstructed weight coefficient after denoising, and the inversion model of denoised Lidar signal and extinction coefficient can be obtained by (9) and (10).

## III. Simulations

We simulate the detection of non-uniform atmosphere using the proposed method, as shown in Fig. 6(a) and (b). It can be seen that within the detection range of 1.5 km, the atmospheric environment exhibits severe non-uniformity, and using the KELL method to estimate boundary value will result in serious error, which will lead to inaccurate inversion results near the boundary values. In contrast, our proposed method can be used to obtain more accurate boundary value of extinction coefficient, which greatly improves the accuracy of non-uniform atmospheric inversion. In addition, we also simulated and analyzed the detection results of two methods for different noise environments. Gaussian white noise is added in the simulation. As shown in Fig. 6(c), the lower the signal-to-noise ratio, the greater the squared mean error(SME) difference between the Lidar and the method proposed in this paper, which is mainly due to the severe error of the boundary values estimated by the KELL method under strong noise. Compared with Lidar method, our method directly measured boundary values to invert the extinction coefficient, thus calculation error is mainly caused by the noise of the signal itself. Especially for the low noise

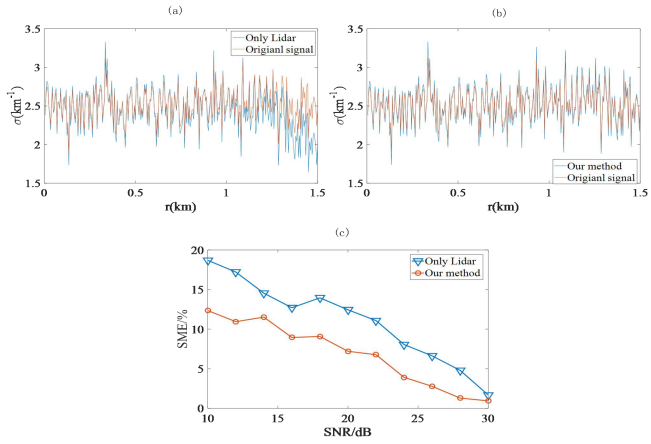


Fig. 6. The inversion results of the extinction coefficient are simulated using Lidar (a) and the method (b) presented in this paper; mean square error of inversion results under different initial signal-to-noise ratios are simulated using the two methods (c).

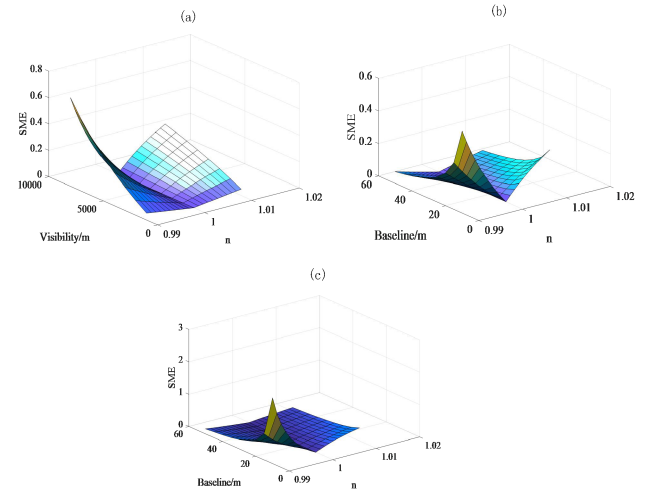


Fig. 7. The relation between visibility, contamination factor and SME is simulated (a) the relations between baseline, contamination factor and SME are simulated under low visibility (b) and high visibility (c).

condition, The inversion results with our method still show good robustness.

According to (1), we regard $n = \eta_i/\eta_0$ as the contamination factor, which can characterize the error ratio caused by lens contamination of the starting and ending points for the mobile measurement system. For transmissive visibility meter, this parameter is the ratio of the error at the laser transmitting end to the one at the receiving end, while for mobile measurement system, it is represented as the ratio of the error at different location of the mobile receiving end. Based on this parameter, we simulate and analyze the impact of mirror contamination on the proposed system under different measurement conditions. As shown in Fig. 7, it can be observed that overall, the closer n is to 1, the smaller the impact of lens contamination on measurement accuracy. Due to the fact that the mobile measurement system only uses the receiving end for sampling, its contamination factor is very close to 1. Therefore, compared with traditional transmissive visibility meter, our method has a better suppression effect on lens contamination. Meanwhile, it can be found that when $n<1$, the contamination impact is much more severe than when $n>1$, and its error will suddenly increase, which is mainly due to the logarithmic operation property in (3). In addition, the impact of contamination factor varies greatly depending on visibility and baseline length. As shown in Fig. 7(a), the higher the visibility, the more severe the impact of lens contamination on the measurement results. Under low visibility (v = 2000), as shown in Fig. 7(b), the shorter the baseline length, the more severe the contamination impact on the measurement results. Under high visibility ($V = 8000$), as shown in Fig. 7(c), a short baseline length can cause serious anomalies in the measurement results, with an error exceeding 100%.

For a long time, the background noise of Lidar has always been an important issue affecting the measurement accuracy of Lidar. To verify the suppression effect of the method proposed in this article on Lidar noise, we simulated four different levels of uniformity in atmospheric environments, as shown in Fig. 8, namely uniform, slightly non-uniform, moderately non-uniform, and severely non-uniform atmospheres. For these four types of atmospheric environments, we constructed Lidar signals with different signal-to-noise ratios and used wavelet analysis, Kalman filtering, empirical mode decomposition, and our method to denoise them. The results are shown in Fig. 9. From it, it can be observed that in Fig. 9(a), the advantages of our method are not significant for a uniform atmospheric environment. However, for the non-uniform atmospheric environment in Fig. 9(c) and (d), our method exhibits significantly better noise suppression effects than the other three methods. Especially for low signal-to-noise ratio situations, such as 10 dB and 15 dB, regardless of atmospheric non-uniformity, this method can improve the denoised signal-to-noise ratio to around 40 dB, demonstrating excellent denoising robustness. This performance is mainly due to the learning coupling effect of precise measurement results on denoising, as well as the adaptive decomposition of empirical mode decomposition for nonlinear and non-stationary signals of Lidar.

## IV. Experiments

To verify the detection effect of the proposed method on non-uniform atmosphere, we firstly placed burning firewood at five locations, including 250 m, 405 m, 665 m, 1025 m, and 1400 m, which can create five points of visibility increasing. Then, detection experiments were conducted on visibility within the range of 1.5 km using the method presented in this article. The time of one measurement satisfies the Taylor freezing hypothesis. As shown in Fig. 10(a), this method can accurately display the positions of five visibility increasing points, and has a good description effect on atmospheric non-uniformity.

Finally, we used a movable forward scattering visibility meter to measure the visibility at nine locations, involving 250 m, 300 m, 405 m, 500 m, 665 m, 800 m, 1025 m, 1300 m, and 1400 m, for comparing the measurement accuracy of our method and the Lidar method. As displayed in Fig. 10(b) and (c),

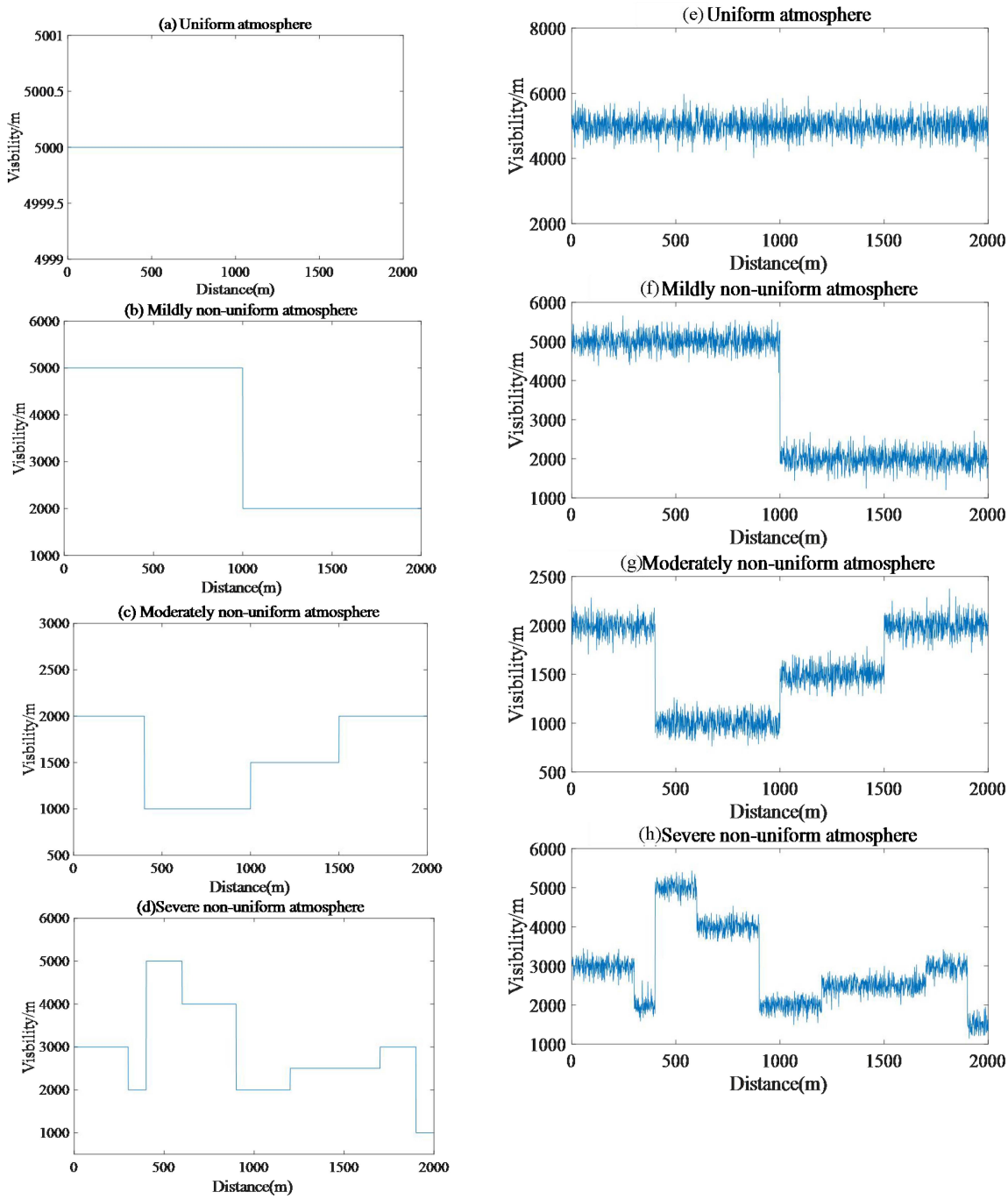


Fig. 8. Atmospheric visibility values of uniform atmosphere (a), mildly non-uniform atmosphere (b), moderately non-uniform atmosphere (c) and severe non-uniform atmosphere (d) are simulated; the visibility inversion results of uniform atmosphere (e), mildly non-uniform atmosphere (f), moderately non-uniform atmosphere (g) and severe non-uniform atmosphere (h) with a signal-to-noise ratio of 25 dB are simulated.

the three measurement results are very close at locations far from the boundary points. However, at locations close to the boundary value points, including 1025 m, 1300 m, and 1400 m, compared to the Lidar method, the proposed method is closer to the measurement results of the forward scattering instrument, demonstrating better measurement accuracy. It is mainly due to the high-precision boundary value measurement in our method.

In order to verify the suppression effect of optical environmental contamination, we conducted continuous experiments for 10000 minutes (7.5 days) with the mobile measurement system and the fixed transmissive one in an indoor environmental simulation cabin at five visibility levels of 500 m, 1500 m, 3000 m, 5000 m, and 8000 m, respectively. During this period, no cleaning or maintenance was carried out on the two types of equipment. Specially, the mobile measurement system performs three mobile measurements per minute in a 30 m baseline, and provides average visibility values per minute; The transmissive visibility meter measures continuously in a 30 m baseline, and

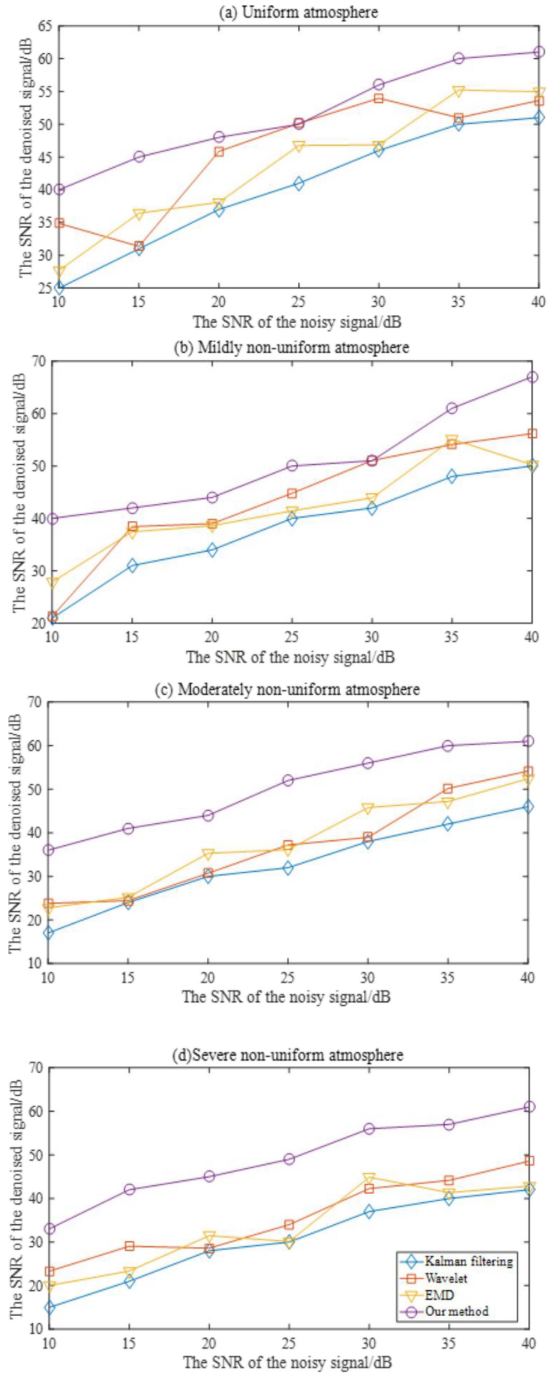


Fig. 9. The denoising results of different method in the environments of uniform atmosphere, mildly non-uniform atmosphere, moderately non-uniform atmosphere, and severe non-uniform atmosphere.

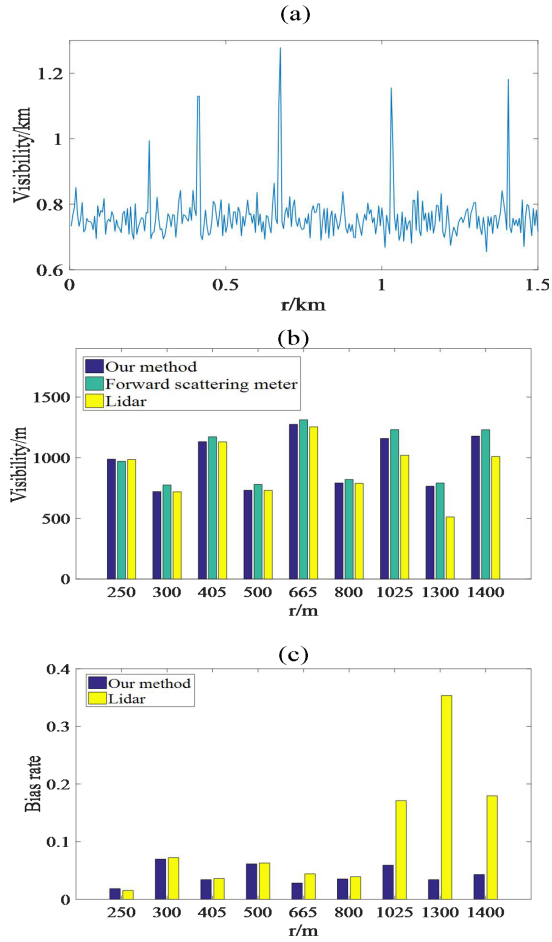


Fig. 10. The visibility of non-uniform atmosphere is measured with our method (a); the measurement results of three methods (b) and bias rate of Lidar and our method (c) compared to forward scattering meter are shown at nine special locations, respectively.

provides an average visibility value per minute. The experiment results are shown in Fig. 11, and it can be observed that as the test duration increases, the deviation between the measurement value and the initial value of transmissive visibility meter becomes larger and larger. This is mainly due to the cumulative effect of optical pollution, and the higher the aerosol concentration in low visibility environments, the more significant the deviation. In contrast, the proposed method has a good suppression effect on optical contamination, with almost no measurement deviation accumulated over time. Especially under low visibility conditions, the test results still have good robustness, for the reason that during the mobile measurement process, the optical contamination error can be offset by measuring the light intensity from the same receiving end.

Finally, to verify the feasibility of this method, we installed and tested the equipment at Civil Aviation University of China near Tianjin Airport, and conducted a visibility testing study for 3 months. The distance between the Lidar and the mobile transmissometer is set to 3 km. With a movement speed of 0.2 meters per second and a residence time of 2 seconds at each interval, the mobile transmissometer can accurately measure the distribution of extinction coefficient in a certain space. By coupling the high-precision measurement values of the transmissometer, the inversion calculation accuracy of the Lidar can be improved. The time of one measurement satisfies the Taylor freezing hypothesis. As shown in Fig. 12, compared with official airport data, it can be seen that the overall measurement results of the joint system are stable and reliable. The low visibility can be accurately detected from August 14th to 16th and September 17th to 18th, with a comparison error of less than 10%.

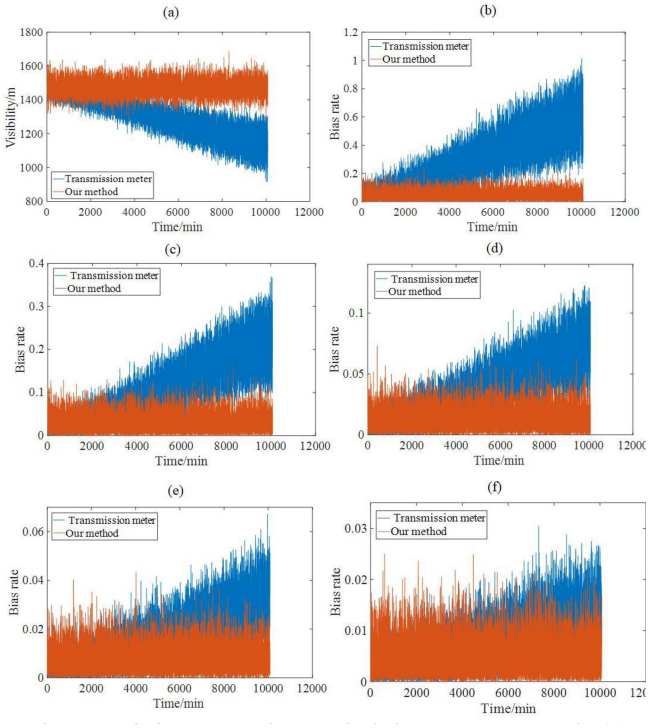


Fig. 11. Using transmission meter and our method, the measurement results (a) and bias rates compared to initial value are shown within 10000 minutes for five visibility levels of 500 m (b), 1500 m (c), 3000 m (d), 5000 m (e), and 8000 m (f).

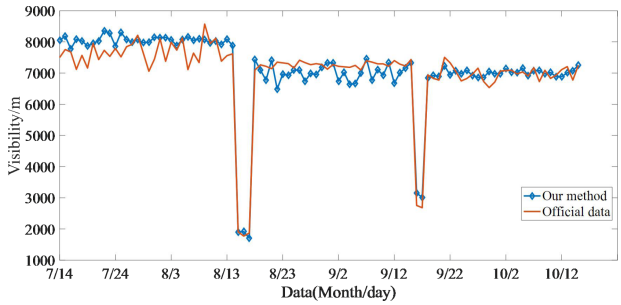


Fig. 12. Experimental testing in airport environments.

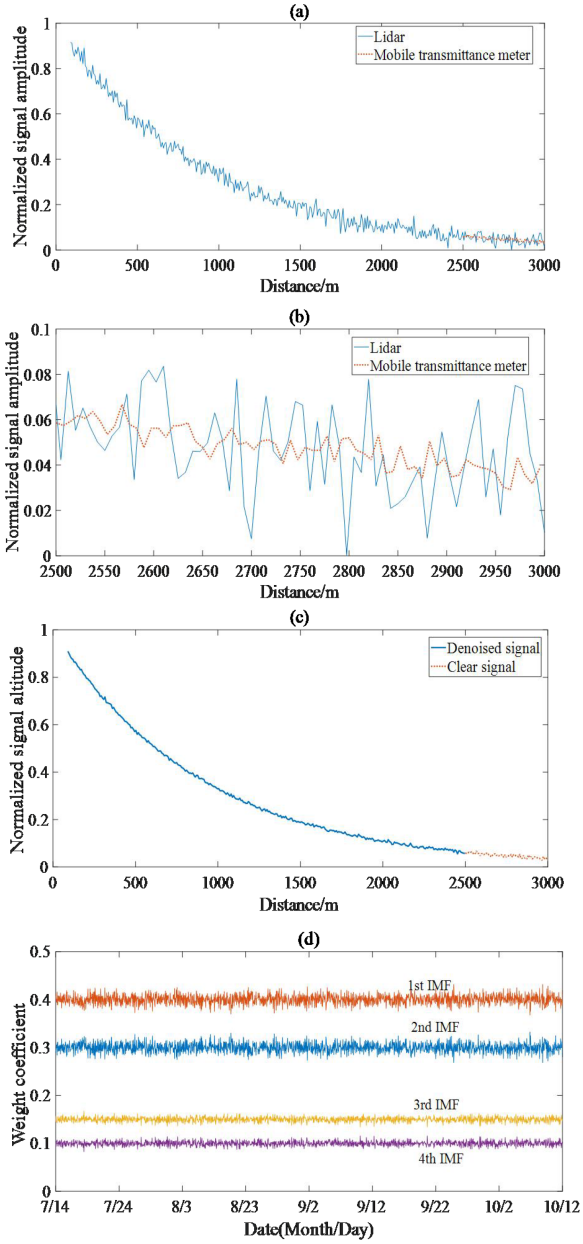


Fig. 13. At 15:00 on July 15th, the original signals of the joint system in large (a) and small (b) scales, the denoised signals (c), and the weight coefficients decomposed within three months (d).

The core goal of signal coupling between Lidar and mobile transmissometer is to effectively denoise Lidar. Fig. 13(a) and (b) show the waveform signals of the Lidar and mobile transmissometer at 15:00 on July 15th. It can be observed that the noise of the Lidar is much greater than that of the mobile transmissometer. Therefore, regarding the signal of the mobile transmission instrument as a clean sample, we can effectively remove the background noise of the Lidar with the learning reconstruction method. As shown in Fig. 13(c), by the proposed learning reconstruction method based on empirical mode decomposition, clear and stable Lidar signal can be obtained, and its overall signal-to-noise ratio is similar to that of the mobile transmissometer. To demonstrate the robustness of the denoising method proposed in this paper, we compare the reconstructed IMF weight coefficients $\omega_k$ at different times, as shown in Fig. 13(d). In Section II-D, the inversion method of Lidar combined mobile transmissometer is used to modify the IMF weight coefficients $\omega_k$, in order to denoise the Lidar signal effectively. Therefore, the distribution characteristics of the IMF weight coefficients $\omega_k$ can effectively demonstrate the stability of denoising. In Fig. 13(d), it can be observed that the larger the scale, the higher the proportion of IMF components. Additionally, regardless of the change in visibility, the weights of the first four IMF components are basically stable, which also indicates that the proposed denoising method based upon learning reconstruction has good generalization ability.

## V. Conclusion

For a long time, the non-uniformity of the atmosphere and environmental pollution caused by optical lenses have always been important issues in high-precision visibility measurement. In response to these issues, we proposed and designed a system that combines the mobile transmissometer with Lidar. This system adopts a mobile sampling method with single receiving end, which can effectively suppress optical contamination caused by atmospheric environment. Simultaneously, combined with Lidar, it can effectively measure the non-uniformity of the atmospheric environment within a specified range. The research results indicate that compared with Lidar, this method has better accuracy near the measurement area of the boundary; compared with the transmissometer, it also exhibits better suppression effect on environmental contamination. Especially in low visibility conditions, our method still has good robustness, which can provide a valuable research direction for high-precision visibility measurement.

## References


[1] A. Ranasinghe, N. Sornkarn, P. Dasgupta, K. Althoefer, J. Penders, and T. Nanayakkara, "Salient feature of haptic-based guidance of people in low visibility environment using hard reins," *IEEE Trans. Cybern.*, vol. 46, no. 2, pp. 568–579, Feb. 2016.

[2] A. Mackin, K. C. Noland, and D. R. Bull, "The visibility estimation and joint inpainting of Lidar depth maps," in *Proc. IEEE Int. Conf. Image Process.*, 2016, pp. 3503–3507.

[3] T. A. Seliga, D. A. Hazen, and L. Salcedo, "Possible enhancements of airport operations based on runway visual range visibility measurements," in *Proc. IEEE/AIAA 28th Digit. Avionics Syst. Conf.*, 2009, pp. 4.E.1-1–4.E.1-13.

[4] P. Peng and C. Li, "Visibility measurements using two-angle forward scattering by liquid droplets," *J. Appl. Opt.*, vol. 55, no. 15, pp. 3903–3908, 2016.

[5] Y. Wu, K. Zhang, Y. Yang, X. Yang, S. Chen, and B. Wang, "Research on forward scattering visibility sensor," in *Proc. IEEE 4th Int. Conf. Automat., Electron. Elect. Eng.*, 2021, pp. 609–612.

[6] Y. Han et al., "Ground-based synchronous optical instrument for measuring atmospheric visibility and turbulence intensity: Theories, design and experiments," *Opt. Exp.*, vol. 26, no. 6, pp. 6833–6850, 2018.

[7] X. Xiong, C. Liu, J. L, M. Li, Y. Ma, and H. Tai, "Effects of multiple scattering on visibility measurement error of laser-transmissometer," *J. Optoelectron. Laser*, vol. 26, no. 10, pp. 2037–2044, 2015.

[8] T. Kaurila, A. Hagard, and R. Person, "Aerosol extinction model based on measurements at two sites in Sweden," *J. Appl. Opt.*, vol. 45, no. 26, pp. 650–6761, 2006.

[9] D. J. Griggs, D. Jones, M. Ouldridge, and W. Sparks, "The first WMO intercomparison of visibility measurements: Final report," Instruments and Observing Methods, World Meteorological Organization, Rep. no. 41, 1990.

[10] P. W. Chan, "A test of visibility sensors at Hong Kong international airport," *Weather*, vol. 71, pp. 241–246, 2016.

[11] S. Waas, "Field test of forward scatter visibility sensors at German airports," in *Proc. WMO Tech.. Conf. Instrum., Methods Observ.*, 2008, pp. 1–17.

[12] R. Nebuloni and E. Verdugo, "FSO path loss model based on the visibility," *IEEE Photon. J.*, vol. 14, no. 2, Apr. 2022, Art. no. 7318609.

[13] I. I. Kim, B. McArthur, and E. Korevaar, "Comparison of laser beam propagation at 785 nm and 1550 nm in fog and haze for optical wireless communications," *Proc. SPIE*, pp. 26–37, 2001.

[14] Q. Wang, L. Bu, T. Li, J. Xu, S. Zhu, and J. Liu, "Alidation of an airborne high spectral resolution Lidar and its measurement for aerosol optical properties over Qinhuangdao, China," *Opt. Exp.*, vol. 28, no. 17, pp. 24471–24488, 2020.

[15] D. K. Kreid, "Atmospheric visibility measurement by a modulated cw Lidar," *Appl. Opt.*, vol. 15, no. 7, pp. 1823–1831, 1976.

[16] W. Gong et al., "Comparison of simultaneous signals obtained from a dual-field-of-view Lidar and its application to noise reduction based on empirical mode decomposition," *Chin. Opt. Lett.*, vol. 9, no. 5, 2011, Art. no. 050101.

[17] H. T. Fang and D. S. Huang D, "Noise reduction in Lidar signal based on discrete wavelet transform," *Opt. Commun.*, vol, vol. 233, no. 1, pp. 67–76, 2004.

[18] F. T. Fang, D. S. Huang, and Y. H. Wu, "Antinoise approximation of the Lidar signal with wavelet neural networks," *Appl. Opt.*, vol. 44, no. 6, pp. 1077–1083, 2005.

[19] F. Mao, W. Gong, and C. Li, "Anti-noise algorithm of Lidar data retrieval by combining the ensemble Kalman filter and the Fernald method," *Opt. Exp.*, vol. 21, no. 7, pp. 8286–8297, 2013.

[20] M. Hu et al., "A novel Lidar signal denoising method based on convolutional autoencoding deep learning neural network," *Atmosphere*, vol. 12, no. 11, 2021, Art. no. 1403.

[21] Z. Hou et al., "Improvement of the signal to noise ratio of Lidar echo signal based on wavelet de-noising technique," *Opt. Lasers Eng.*, vol. 51, no. 8, pp. 961–966, 2013.

[22] S. Wu, Z. Liu, and B. Liu, "Enhancement of Lidar backscatters signal-to-noise ratio using empirical mode decomposition method," *Opt. Commun.*, vol. 267, no. 1, pp. 137–144, 2006.

[23] P. Tian et al., "Improved empirical mode decomposition based denoising method for Lidar signals," *Opt. Commun.*, vol. 325, pp. 54–59, 2014.

[24] L. H. Jiang, F. Chao, W. Q. Liu, and X. L. Xiong, "Lidar backscattering signal denoising method based on adaptive multi-scale morphological filtering and EMD," *Infrared Laser Eng.*, vol. 44, no. 05, pp. 1673–1679, 2015.

[25] J. Chang et al., "Noise reduction in Lidar signal using correlation-based EMD combined with soft thresholding and roughness penalty," *Opt. Commun.*, vol. 407, pp. 290–295, 2018.

[26] Y. Z. Ma et al., "Laser radar signal denoising algorithm based on CEEMD combined with improved wavelet threshold," *Syst. Eng. Electron.*, vol. 45, no. 1, pp. 93–100, 2023.

[27] J. D. Klett, "Stable analytical inversion solution for processing Lidar returns," *Appl. Opt.*, vol. 20, no. 2, pp. 211–220, 1981.

[28] X. L. Xiong, L. H. Jiang, S. Feng, and Z. B. Zhuang, "Determination of the boundary value of atmospheric aerosol extinction coefficient based on fixed point principle," *J. Optoelectron.·Laser*, vol. 23, no. 2, pp. 303–309, 2012.

[29] X. L. Xiong et al., "Using improved Newton method to determine the boundary value of atmospheric extinction coefficient," *Infrared Laser Eng.*, vol. 41, no. 07, pp. 1744–1749, 2012.

[30] G. D. Sun et al., "A new method of measuring boundary value of atmospheric extinction coefficient," *Acta Physica Sinica*, vol. 67, no. 5, pp. 148–155, 2018.

[31] J. Xian, D. Sun, S. Amoruso, W. Xu, and X. Wang, "Parameter optimization of a visibility Lidar for sea-fog early warnings," *Opt. Exp.*, vol. 28, no. 16, pp. 23829–23845, 2020.

[32] J. Shen and N. W. Cao, "Inversion of tropospheric aerosol extinction coefficient profile by Mie-Raman scattering Lidar," *Chin. J. Lasers*, vol. 44, no. 6, pp. 304–313, 2017.

[33] Y. C. Zhang, S. Chen, and W. S. Tan, "Inversion algorithm of aerosol backscattering coefficient with water cloud particle backscattering coefficient as boundary value," *Acta Optica Sinica*, vol. 42, no. 24, pp. 179–188, 2022,.

[34] J. Wang, "Research on the method of visibility inversion based on Lidar joint detection," Civil Aviation University of China For the Academic Degree of Master of Science, pp. 36–47, 2020.

[35] R. Nebuloni, "Empirical relationships between extinction coefficient and visibility in fog," *Appl. Opt.*, vol. 44, 2005, Art. no. 3795.